Catalysis Today 175 (2011) 380–385

Contents lists available at ScienceDirect

Catalysis Today

journal homepage: www.elsevier.com/locate/cattod

Co-SBA-15 for heterogeneous oxidation of phenol with sulfate radical for wastewater treatment

Pradeep Shukla, Hongqi Sun, Shaobin Wang*, H. Ming Ang, Moses O. Tadé

Department of Chemical Engineering and Cooperative Research Centre for Contamination Assessment and Remediation of the Environment (CRC-CARE), Curtin University, GPO Box U1987, Perth, WA 6845, Australia

ARTICLE INFO

Article history:
Received 14 October 2010
Received in revised form 24 February 2011
Accepted 1 March 2011
Available online 31 March 2011

Keywords:
SBA-15
Phenol degradation
Sulfate radical
Advanced oxidation

ABSTRACT

Mesoporous silica SBA-15 supported cobalt catalysts were prepared by co-condensation during SBA-15 synthesis, using three different Co(II) precursor salts, chloride (Cl), acetate (Ac) and nitrate (N). The physicochemical properties of the catalysts were characterized by several techniques, such as XRD, SEM (EDS), TEM, and FT-IR. It was found that Co_3O_4 was formed in SBA-15 and would effectively activate peroxymonosulfate to produce sulfate radicals for phenol oxidation in heterogeneous solutions. The Co precursors affected the physicochemical property, activity and stability of the catalysts. In heterogeneous reactions, the effects of catalyst loading, peroxymonosulfate concentration and reaction temperature on phenol degradation were investigated. The heterogeneous phenol degradation reactions followed zero order kinetics and the activation energies were 81.4, 67.4 and 67.4 kJ/mol for Co/SBA-15-Cl, Co/SBA-15-Ac, and Co/SBA-15-N, respectively.

1. Introduction

In the past few decades there has been an extensive increase in urbanization and industrialization around several parts of the world. On one hand, this has significantly improved the living standard of people, on the other hand it has added excessive burden on the natural resources, especially clean water. Excessive consumption of water and discharge of wastewater from various industrial processes and domestic households have posed risks to sustainable availability of this natural resource, thus making it imperative to develop technologies to treat and recycle the discharged wastewater streams. Extensive investigations have been made to develop an effective strategy to treat wastewater, such as adsorption, filtration, flocculation, chemical precipitation and membrane separation, etc. However, most of these processes just transfer the pollutants from one phase (liquid) to another (solid), rather than completely destroy the organic contaminants in water. New technologies for the complete destruction of aqueous organics as well as deep water purification for drinking water are still being highly demanded. Recently, several advanced oxidation processes (AOPs) have been proposed by many researchers and proven to be practically feasible for removal of organic pollutants [1–4].

In general, most of AOPs employ active radicals which are extremely reactive and readily attack organic pollutants, thereby transforming them into harmless end products such as CO_2 and H_2O. The type and strength of the active radicals depend on the oxidant employed in the process. Oxidation by the Fenton reagents, Fe^{2+} or Fe^{3+} ions with hydrogen peroxide, has been used successfully for decades [5,6]. Such processes, sometimes, are restricted by acidic pH requirement (pH 2–4), generation of high amount of sludge in coagulation step, and loss of Fe ions in water. The need for a more convenient AOP process has encouraged the investigation of other oxidizing reagents. Many investigations have reported that sulfate radicals, generated from peroxymonosulfate (PMS) in the presence of a cobalt catalyst, can be effective for oxidation of phenolic compounds [7–9]. The radical generation and the degradation processes can be described as below.

$$Co^{2+} + HSO_5^- \rightarrow Co^{3+} + SO_4^{\bullet -} + OH^- \quad (1)$$

$$SO_4^{\bullet -} + C_6H_5OH \rightarrow C_6H_5OH\text{–}SO_4^{\bullet -} \rightarrow C_6H_5OH^{\bullet +} + SO_4^{2-} \rightarrow \text{severalsteps} \rightarrow CO_2 + H_2O + SO_4^{2-} \quad (2)$$

Co^{2+}/PMS system works like a modified Fenton reaction (Fe^{2+}/H_2O_2). Due to higher oxidation potential of sulfate radical [2.5–3.1 eV] as compared to hydroxyl radical [2.7 eV], much faster reaction rate in oxidation can be achieved in sulfate radical process than in Fenton oxidation. However, the major issue confronting cobalt based oxidation technique is the toxicity of cobalt ion. Cobalt is recognized as a priority pollutant in water, which leads to several health problems such as asthma, pneumonia and other lung problems. In order to restrict the discharge of cobalt ions, it has been

* Corresponding author. Tel.: +61 8 92663776; fax: +61 8 92662681.
E-mail address: Shaobin.wang@curtin.edu.au (S. Wang).

0920-5861/$ – see front matter © 2011 Elsevier B.V. All rights reserved.
doi:10.1016/j.cattod.2011.03.005

proposed to employ a heterogeneous cobalt catalyst by supporting the cobalt ions on a solid surface for oxidation.

Several supports have been investigated for encapsulation of cobalt ions to carry out the heterogeneous reaction in the presence of PMS. Cobalt ion-exchange in ZSM-5 has been reported as an efficient catalyst, however, the reaction rate is limited by lower amount of cobalt ions being exchanged in the unit cell [9]. Higher amount of cobalt can be loaded into the pores of silica, alumina or titania supports by impregnation thus resulting in faster reactions [10], however, the nonuniform and smaller pore structure of the supports result in non-uniformed distribution of catalyst. Since the discovery of ordered mesoporous silica materials in 1990s, synthesis and applications of the mesoporous solids have received an intensive attention due to their highly ordered structure, larger pore size, and high surface area [11,12]. The large pore size and high pore volume favor catalyst loading and uniform dispersion thus enhancing the effectiveness of the catalyst. In the past few years, some heterogeneous Co catalysts were reported for advanced oxidation using sulfate radical including Co oxides [7,13] and supported Co oxides [10,14–16]. However, very limited investigations have been reported in mesoporous silica supported Co oxides for heterogeneous oxidation [9,17].

In this paper, Co/SBA-15 was prepared by co-condensation of cobalt during SBA-15 synthesis. SBA-15 has a well-ordered hexagonal mesoporous structure with uniform pore sizes up to approximately 30 nm and BET surface areas up to 1000 m^2/g [18]. It was proposed that loading cobalt into the pore structure of SBA-15 would not only hinder the cobalt leaching but also improve the reaction efficiency by using the good adsorption performance of the mesoporous silica. This combined technique would be much efficient than the popular TiO_2-photocatalysis, and would manage to completely destruct organic pollutants comparing to the traditional adsorption on SBA-15. The as-prepared catalysts, derived from three different cobalt precursors, were utilized to activate PMS for oxidation of aqueous phenol solutions. The effects of Co precursor and oxidation conditions were systematically investigated.

2. Experimental

2.1. Synthesis of cobalt/SBA-15 catalysts

A mesoporous silica SBA-15 was prepared following the procedure described by Zhao et al. [18] using a tri-block copolymer, poly(ethylene glycol)-block-poly(propylene glycol)-block-poly(ethylene glycol), EO_{20}-PO_{70}-EO_{20}, as a template agent and tetraethyl orthosilicate (TEOS) as a silica source, respectively. In a typical synthesis, 12 g of tri-block copolymer and 13.44 g of KCl were dissolved in 360 mL of 2 M HCl solution with stirring at 40 °C and then 22.96 g of TEOS was added into the solution with vigorous stirring for 8 min. The mixture was kept aging under static condition for 24 h at the same temperature. The resulted mixture was transferred to an autoclave and kept at 100 °C for 24 h. The SBA-15 silica product was then filtered, washed with distilled water and dried at 50 °C. The polymeric structure-directing agent (EO_{20}-PO_{70}-EO_{20}) was removed by calcination at 550 °C for 6 h in air.

Cobalt chloride ($CoCl_2$), acetate ($Co(CH_3COO)_2$), and nitrate ($Co(NO_3)_2$) obtained from Sigma-Aldrich Chemicals were used as the precursors of cobalt ions. During the preparation of SBA-15, some amounts of three Co precursors was dissolved in the solution just after the addition of TEOS to obtain 5 wt% Co in the sample for co-condensation of Co and silica. The three catalysts are labeled as Co/SBA-15-Cl (from cobalt chloride), Co/SBA-15-Ac (from cobalt acetate), and Co/SBA-15-N (from cobalt nitrate), respectively.

2.2. Characterization of catalysts

The catalysts were characterized using several techniques to identify the structural and physicochemical properties. The crystalline form of the catalysts was identified by X-ray diffractometer (XRD) on a Bruker D8 advanced research XRD with Cu Kα radiation at a scanning rate of 2°/min. Scanning electron microscopy (SEM), performed on a Zeiss Neon 40EsB FIBSEM, was employed to investigate the texture and morphology of the samples. The energy dispersive spectroscopy (EDS) and the elemental (Co) mapping were also carried out to detect the distribution of Co in the sample. The mesoporous structures of the samples were further confirmed by transmission electron microscopy (TEM) operated on a JEOL 2011 TEM instrument. The Fourier transform infrared (FTIR) spectra were acquired on a Bruker instrument using a KBr pellet technique at room temperature. The dried KBr was homogenized with the samples in a mortar. The disks with 1 cm in radius and thickness of 0.1 cm were then prepared using a hydraulic presser. All the spectra were recorded over 4000–400 cm^{-1} at a resolution of 4 cm^{-1}.

2.3. Kinetic study of phenol oxidation

The catalytic oxidation of phenol was carried out in a 500 mL reactor containing 30 ppm of phenol solution. The reactor was attached to a stand and dipped in a water bath with a temperature controller. The reaction mixture was stirred constantly to maintain a homogeneous solution. A known amount of oxidant, oxone (peroxymononsulfate, $2KHSO_5{\cdot}KHSO_4{\cdot}K_2SO_4$) obtained from Aldrich, was added to the mixture and allowed to dissolve before the reaction. Later some quantity of catalysts depending on the predefined reaction parameter was added in the reactor to start the reaction. The reaction was continuously carried out for 6 h. At a fixed interval, 0.5 mL sample was withdrawn using a syringe filter into a HPLC vial. A 0.5 mL methanol solution was immediately added to quench the reaction. The concentration was analyzed using a HPLC (from Varian Instrument) with a UV detector at the wavelength of 270 nm. The column used was C-18 and the mobile phase was 30% CH_3CN and 70% water.

After reaction, the spent catalysts were recovered from the reaction mixture by filtration and washed thoroughly with distilled water and dried at 70 °C for reuse.

3. Results and discussion

3.1. Characterization of Co/SBA-15 catalysts

Fig. 1 shows XRD spectra of SBA-15 support and Co/SBA-15 catalysts, which were prepared by different precursors. For SBA-15, a big broad peak was observed at around 22°, which is commonly appearing for amorphous supports. For Co/SBA-15-Cl and Co/SBA-15-Ac, apart from the broad peak at 22°, several strong peaks at 18.7°, 31.1°, 36.7°, 38.4°, 44.6°, 55.4°, 59.2° and 65.0° were also observed. These peaks were assigned to Co_3O_4 crystallites at the crystal faces of [111], [220], [311], [222], [400], [422], [511] and [440], respectively. Other weak signals possibly suggest the presence of CoO [19]. The crystal phases of cobalt oxides in the sample of Co/SBA-15-N were different from the above samples. As shown by curve (b) of Fig. 1, the peaks were identified as mixed phases of CoO, Co_2O_3, and Co_3O_4. Based on the XRD profiles, the crystal sizes of these cobalt oxides were estimated by the Scherrer equation: $D = K\lambda/(B\cos\theta)$. The crystal size of Co_3O_4 in Co/SBA-15-Cl was 14.0 and 6.7 nm in Co/SBA-15-Ac. In Co/SBA-15-N, CoO was 2.8 nm, Co_2O_3 was 1.7 nm, and Co_3O_4 was too small to be estimated.

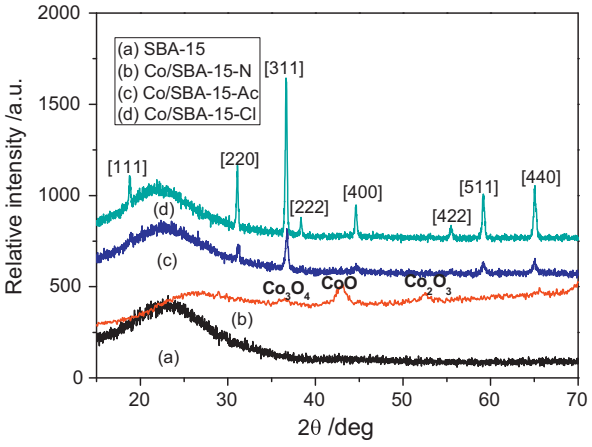

Fig. 1. XRD patterns of SBA-15 and Co/SBA-15 catalyst.

Fig. 2 presents the small angle XRD spectra of SBA-15 and Co/SBA-15 catalyst. Three peaks at 1.057°, 1.559°, and 1.844° were found in SBA-15 sample, representing the planes of [1 0 0], [1 1 0] and [2 2 0], respectively, and they conform to the *p6mm* space group for hexagonal arrays of mesopores. The similar peaks were found to be slightly less resolved in the case of Co/SBA-15, suggesting the similar mesoporous structure as SBA-15.

Fig. 3 displays SEM image, EDS and Co mapping of Co/SBA-15 catalyst. The SBA-15 particles were observed to be rod-like cylindrical beads with the particle size at 1–3 microns. EDS profile shows that carbon, oxygen, aluminum, silicon, platinum and cobalt exist in the sample. Carbon was from contamination, aluminum from the stub used for holding sample, and platinum from coating. Inset of Fig. 3(B) displays the cobalt mapping, which was used to detect Co and evaluate its distribution. It was seen that Co was uniformly dispersed in the selected area except for little amount of aggregation represented by the larger bright dots in the image. The TEM images, as shown in Fig. 4, were employed to confirm the well-defined channels in both SBA-15 and Co/SBA-15, and the results were consistent with the small angle XRD. The results confirmed the mesoporous structures of the SBA-15 support and Co/SBA-15 catalyst. [20] This suggests that Co/SBA-15 prepared by co-condensation of metal and silica will maintain the mesoporous structure.

Fig. 5 shows FT-IR spectra of Co/SBA-15 prepared by three different Co precursors. A major peak at 1066 cm^{-1} represents the

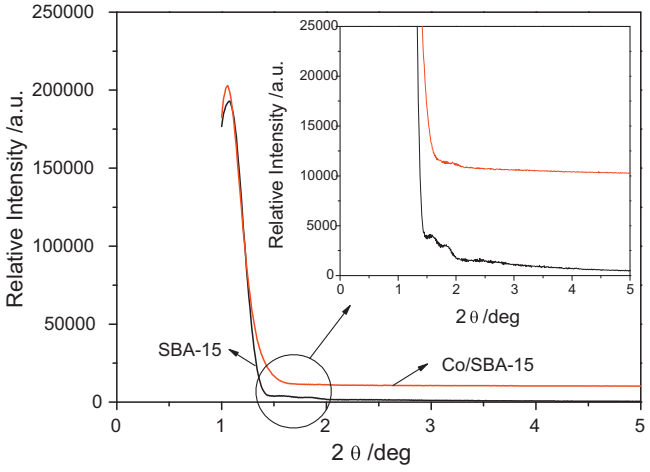

Fig. 2. Small angle XRD spectra of SBA-15 and Co/SBA-15, inset: magnification of weak peaks.

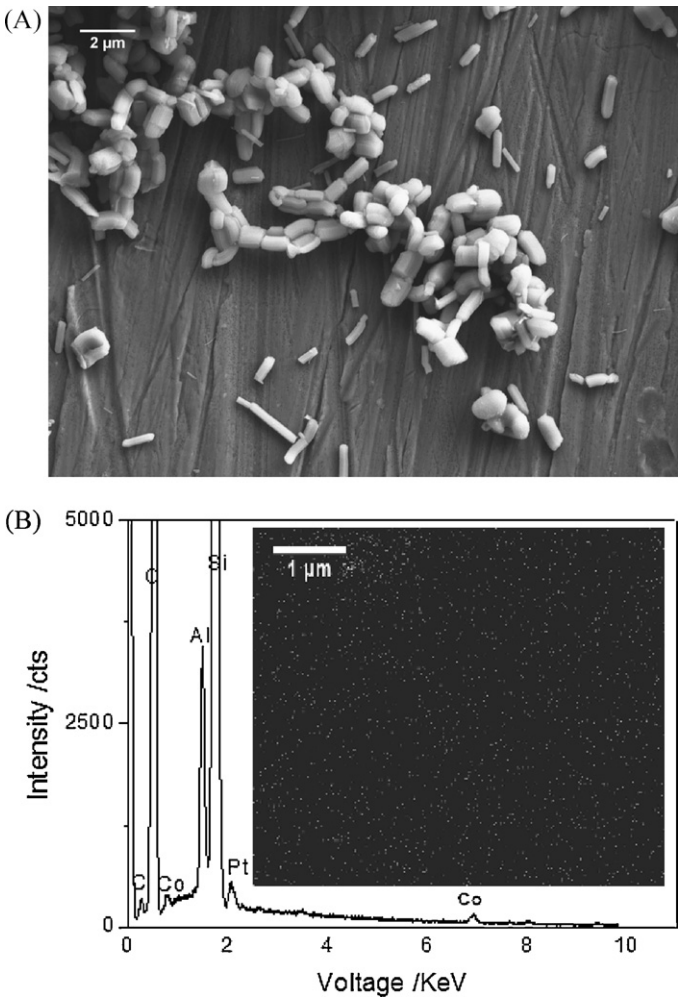

Fig. 3. SEM image (A), EDS and Co mapping (B) of Co/SBA-15-Cl catalyst.

IR absorption due to stretching of Si–O–Si. The peaks close to 450 and 750 cm^{-1} were observed due to the bending and asymmetric stretching of the silicon and oxygen bonds. A small peak observed at around 1600 cm^{-1} is attributed to the presence of silanol (Si–OH) group. This functional group is formed during the hydrolysis reaction of TEOS in the aqueous solution. The broad peak at 3357 cm^{-1} represents the O–H vibrations, which would arise from the adsorbed water molecules on the surface [21]. A very small shoulder around 568 cm^{-1} was found in each sample. This signal is attributed to the presence of spinal Co–O bonding, suggesting the presence of small quantity of cobalt oxide crystallites [22].

3.2. Catalytic activity of phenol degradation on Co/SBA-15 catalysts

Control experiments were conducted in order to examine the effectiveness of cobalt loaded SBA-15 for phenol degradation under the influence of oxone. Fig. 6 shows the dynamic degradation of phenol with Co/SBA-15 catalyst and oxone. For the reaction carried out in the presence of oxone without any catalyst, negligible change in phenol concentration was observed. A change of less than 5% in phenol concentration was found after 400 min, suggesting that the oxone itself in homogeneous solution could not induce significant oxidation of phenol. A similar observation was made in the reaction carried out with the catalyst alone, indicating that the catalyst did not exhibit strong adsorption of phenol. For Co/SBA-15 with oxone in the heterogeneous system, phenol concentration grad-

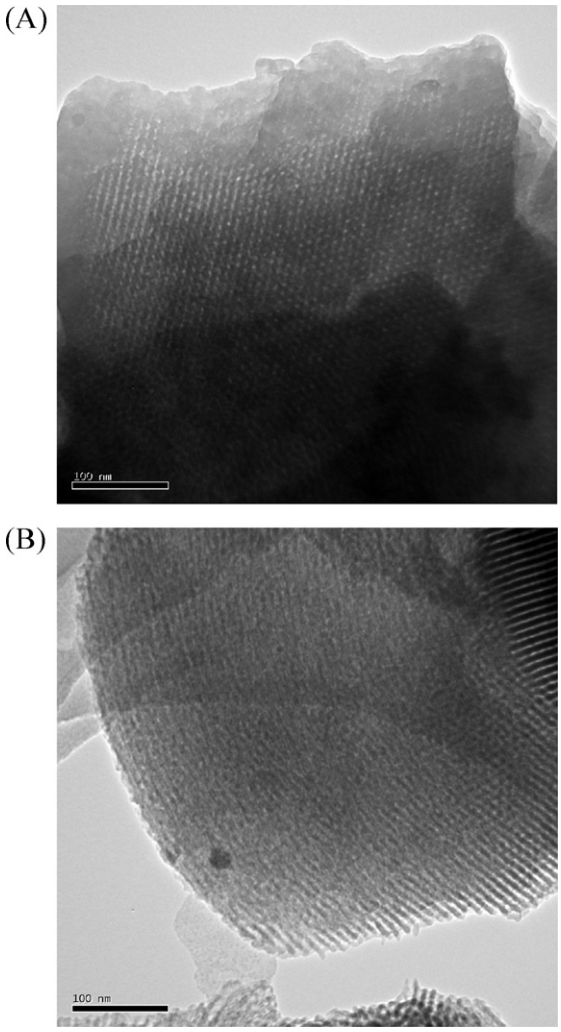

Fig. 4. TEM images of SBA-15 (A) and Co/SBA-15-Cl catalyst.

ually decreased and the degradation rate seemed to be constant and 100% phenol removal could be achieved in 180 min. The high degradation rate was due to the activation of PMS by Co_3O_4 to produce sulfate radicals. The reaction mechanisms for heterogeneous phenol oxidation can be proposed as follows.

$$S\text{-}Co^{3+} + HSO_5^- \rightarrow S\text{-}Co^{2+} + SO_5^{\bullet -} + H^+ \quad (S\text{-solid}) \qquad (3)$$

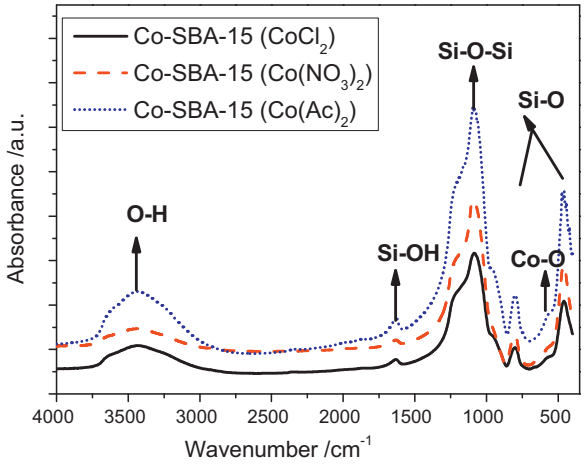

Fig. 5. FTIR spectra of three Co/SBA-15 samples.

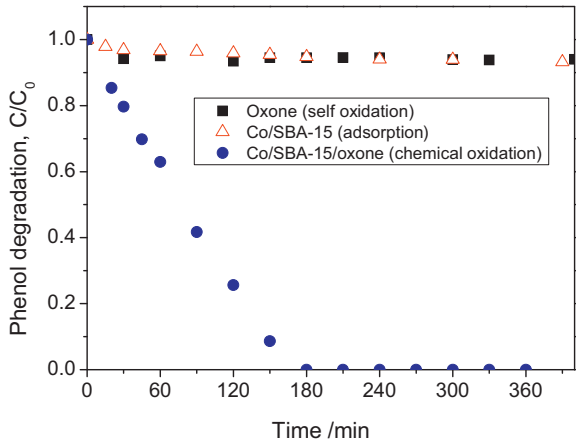

Fig. 6. Oxidation of phenol at different conditions. [phenol: 30 ppm, $T = 25\,^{\circ}C$, catalyst loading: 0.2 g/L, and oxone: 2 g/L].

$$S\text{-}Co^{2+} + HSO_5^- \rightarrow S\text{-}Co^{3+} + SO_4^{\bullet -} + OH^- \quad (\text{slow}) \qquad (4)$$

$$SO4^{\bullet -} + C_6H_5OH \rightarrow SO_4^{2-} + C_6H_5O^{\bullet} + H^+ \quad (\text{fast}) \qquad (5)$$

Compared with the efficiency of Co^{2+} ions/PMS system in homogeneous oxidation, the heterogeneous degradation efficiency was found to be lower, however, previous results by cobalt oxide or supported cobalt seemed to be feasible for practical application with acceptable efficiency. [4,7,10,23]

Fig. 7 shows that the cobalt precursors would significantly influence the activity of the Co/SBA-15 catalysts. The catalysts derived from cobalt chloride and acetate demonstrated similar activities, and they would achieve 100% phenol removal in 200 min. However, the reaction rate of Co/SBA-15-N was much slower, reaching 100% removal in 390 min. The highest activity of Co/SBA-15-Cl was possibly attributed to the loose connection of Co to the SBA-15. As shown before, the crystallite size (14.0 nm) of Co_3O_4 in Co/SBA-15-Cl was too big to be incorporated into the mesopore structure (ca. 9 nm) of SBA-15. Thus, the exposed Co_3O_4 would become easily and efficiently react with PMS than those inside SBA-15 pores. Yang et al. [10] investigated catalytic activity of several Co/TiO_2 catalysts prepared from Co precursors of nitrate, sulfate (S) and chloride in degradation of 2,4-dichlorophenol in water. They found that the activities of the three Co/TiO_2 catalysts were in accordance with their cobalt leaching, in an order of Co/TiO_2-S > Co/TiO_2-Cl > Co/TiO_2-N. Moreover, Co/TiO_2-N possessed smaller crystalline size and better cobalt dispersion than Co/TiO_2-Cl due to

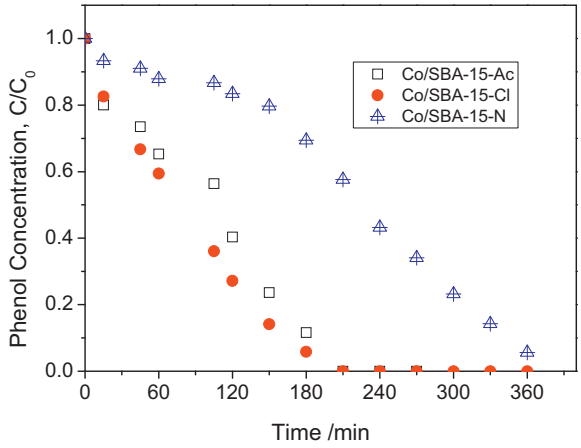

Fig. 7. Effect of cobalt precursor on the efficiency of phenol oxidation. [phenol: 30 ppm, $T = 25\,^{\circ}C$, catalyst loading: 0.2 g/L, and oxone: 2 g/L].

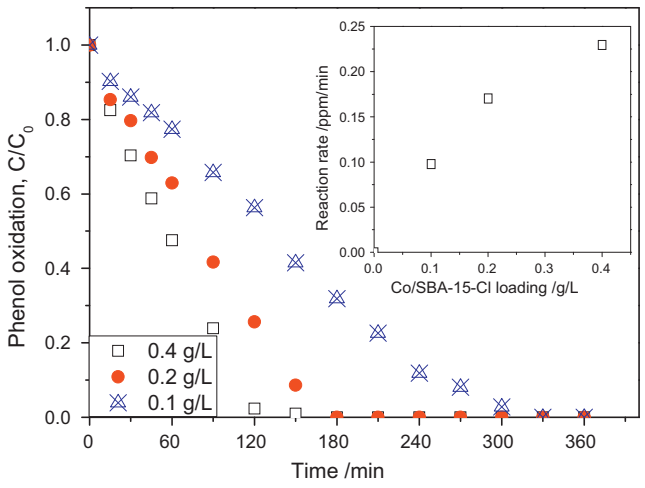

Fig. 8. Effect of catalyst loading on the phenol degradation and its zero-order kinetics. [phenol: 30 ppm, T = 25 °C, and oxone: 2 g/L].

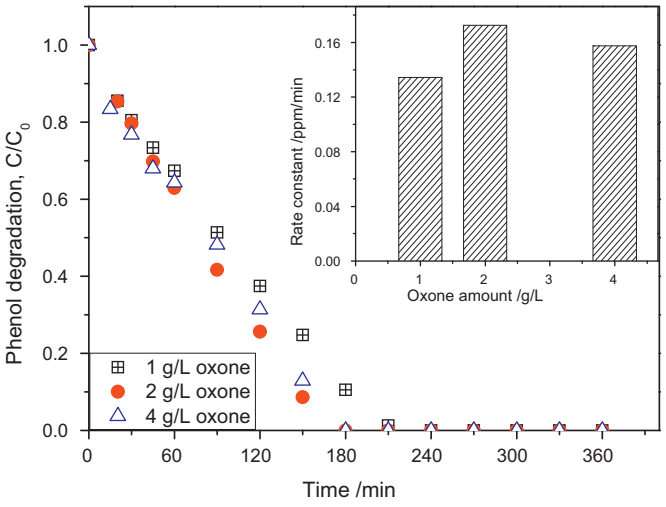

Fig. 9. Effect of oxidant amount on the phenol degradation and its zero-order kinetics. [phenol: 30 ppm, T = 25 °C, and catalyst loading: 0.2 g/L].

its smaller pore size. Their results were similar to the observations in this investigation.

Due to the highest activity, further kinetic studies on Co/SBA-15-Cl were conducted in the investigation. Fig. 8 displays phenol degradation on Co/SBA-15 with oxone at varying catalyst loading. Higher Co/SBA-15 loading in solution resulted in higher phenol degradation rate and efficiency. At 0.1 g/L of Co/SBA-15, phenol degradation would reach 100% in 330 min while the time would be decreased to be 180 min at 0.2 g/L loading of Co/SBA-15. The duration would be further reduced to be 120 min when increasing catalyst loading at 0.4 g/L. The increased efficiency is clearly attributed to the increased availability of active sites in the solution for reaction with PMS thereby generating more sulfate radicals. Inset of Fig. 8 displayed that the reaction rate increased with catalyst loading. The kinetics of organic degradation in cobalt/oxone varied with reaction conditions. A pseudo first-order decolorization was proposed by Chen et al. [24] in acid orange 7 (AO7) degradation in aqueous Co^{2+}/oxone. A second-order kinetics for acid red 183 (AR183) degradation was reported by Ling et al. [23] in the investigation of Co^{2+}/oxone oxidation of dyes. We previously reported the zero-order kinetics in heterogeneous degradation of phenol on Co-zeolite system. [9] In this study the zero-order model still fit well to the experimental data with high regression coefficients. In present batch study, the amount of cobalt catalyst was fixed. The zero order kinetics of the reaction suggests the generation of active radical as the rate controlling step rather than the phenol degradation.

Fig. 9 illustrates the effect of oxone concentration on phenol oxidation. The influence was not as significant as catalyst loading. The degradation rate was increased 28% when oxone concentration was increased from 1 to 2 g/L. However, further increase in oxone concentration would result in lower degradation efficiency and rate constant. A 16% loss in phenol oxidation rate would occur when the oxone concentration was increased to 4 g/L from 2 g/L. This was possibly due to the self-quenching of sulfate and hydroxyl radicals by PMS as follows [25].

$$HSO_5^- + SO_4^{\bullet -} \rightarrow SO_5^{\bullet -} + SO_4^{2-} + H^+ \quad (6)$$

$$HSO_5^- + OH^\bullet \rightarrow SO_5^{\bullet -} + H_2O \quad (7)$$

The chemical composition of oxone is $2KHSO_5{\bullet}KHSO_4{\bullet}K_2SO_4$. The reduction potential of $SO_5^{\bullet -}/HSO_5^-$ is E_7 = 0.95 V at pH 7, E_4 = 1.12 V at pH 4, and E_2 = 1.24 V at pH 2. Meanwhile, $SO_4^{\bullet -}/SO_4^{2-}$ has an oxidation potential of [2.5–3.1 V], which makes it possible that higher concentration of HSO_5^- from oxone at higher concentration would consume the active $SO_4^{\bullet -}$, resulting in a lower degradation rate.

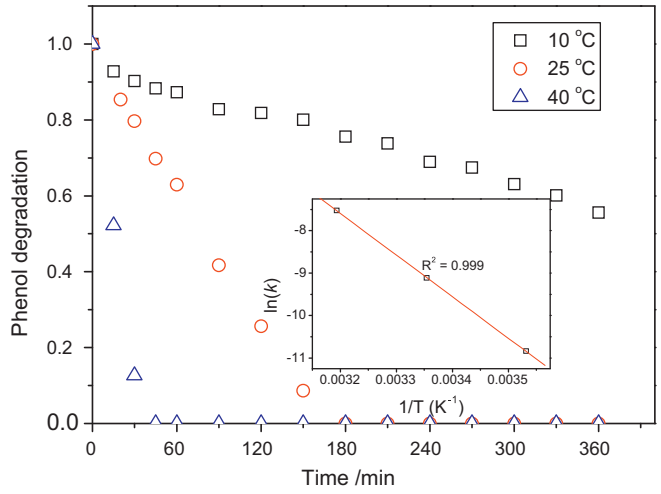

Fig. 10. Effect of reaction temperature on the phenol degradation and its zero-order kinetics. [phenol: 30 ppm, catalyst loading: 0.2 g/L, and oxone: 2 g/L].

Fig. 10 reveals that phenol degradation also depended on reaction temperature. It was seen that reaction temperature dramatically affected oxidation efficiency and degradation rate. At 10 °C, only 40% of phenol would be decomposed in 360 min, while 100% phenol removal was achieved when increasing the temperature to 25 °C. When reaction temperature reached 40 °C, phenol would be completely destructed in 45 min.

From the zero order kinetic model, the apparent reaction rate constants were obtained and they were well related with temperature by the Arrhenius equation. Table 1 lists the activation energy of the Co/SBA-15 catalysts prepared by different cobalt precursors. Previous investigations showed that phenol degradation on Co/ZSM5 and Co/AC has the activation energy of 69.7

Table 1
Activation energy of phenol degradation on various Co/SBA-15 catalysts.

Catalyst	Activated energy (E_a, kJ/mol)	Regression coefficient (R)
Co/SBA-15-Cl	81.4	0.999
Co/SBA-15-Ac	67.4	0.998
Co/SBA-15-N	67.4	0.991

Table 2
Rate constant of the zero order kinetics of phenol degradation on various Co/SBA-15 catalysts.

Catalyst	Rate constant (ppm/min)	Regression coefficient (R)
Co/SBA-15-Cl (1st run)	0.1725	0.999
Co/SBA-15-Cl (2nd run)	0.0232 (decreases 86.6%)	0.978
Co/SBA-15-Ac (1st run)	0.1295	0.991
Co/SBA-15-Ac (2nd run)	0.0714 (decreases 44.9%)	0.990
Co/SBA-15-N (1st run)	0.0741	0.994
Co/SBA-15-N (2nd run)	0.0651 (decreases 12.1%)	0.995
Co/SBA-15-N (3rd run)	0.0569 (decreases 23.2%)	0.996

[9] and 59.7 kJ/mol [16], respectively. It is noteworthy that the activation energy only gives the dependence of reaction rate on the reaction temperature, and it cannot be related to the activity of catalysts before obtaining the identical pre-exponential factors.

It is known that the stability of the catalyst is more important in practical application. In Co/SBA-15/oxone system, the activity loss was mostly due to cobalt leaching [7,13]. Previous studies of supported cobalt catalysts for activation of oxone have indicated varying stability of the catalysts. Chu et al. [26] reported that the reusability of the supported cobalt depended on the supports. Co/Zeolite showed poor stability and degradation efficiency of Monuron remained only 30% at the second run. Zhang et al. [14] found that the activity of Co/MgO for dye decomposition dropped slightly in three runs. We previously showed that Co/ZSM-5 remained unaffected in the second run and decreased slightly in the third run, but Co/Zeolite-A showed very poor stability [9].

Table 2 lists the rate constant of phenol degradation of Co/SBA-15 catalysts and regression coefficient of the model fitting. For Co/SBA-15-Cl, the rate constant reduced 86.6% at the second run. As shown before, this catalyst presented the highest efficiency among the three catalysts, possibly due to the looser connection of cobalt with SBA-15 matrix. For Co/SBA-15-Ac, 44.9% efficiency would be lost at the second run, showing higher stability than Co/SBA-15-Cl. The cobalt leaching was suggested to be responsible for the decreased activity in reuse. The leaching was found to be dependent on the concentration of PMS and 8.14%, 18.26% and 20.73% of cobalt were leached after the reactions at the PMS concentrations of 1, 2 and 3 g/L, respectively. The Co/SBA-15-N exhibited the highest stability among the samples, at the second run only 12.1% activity was lost, and at the third run, 76.8% activity still maintained. It is recalling that, as shown in Fig. 7 and Table 2, Co/SBA-15-N provided lower activity, thus we proposed that the lower activity was due to fine crystallites deepened into SBA-15 matrix, resulting in less cobalt leaching.

4. Conclusion

Co/SBA-15 was an effective catalyst in heterogeneous activation of oxone for phenol oxidation in aqueous solution. The major Co species on Co/SBA-15 was detected to be Co_3O_4. The cobalt precursors, $CoCl_2$, $Co(CH_3COO)_2$ and $Co(NO_3)_2$, significantly affected the activity and stability of the catalysts. The rate constant of the catalysts followed an order of Co/SBA-15-Cl > Co/SBA-15-Ac > Co/SBA-15-N, and the reusability followed an opposite tendency. The difference was attributed to the varying bonding of cobalt to SBA-15. Phenol degradation was greatly influenced by catalyst loading and higher catalyst loading in solution would increase phenol degradation. Meanwhile, oxone concentration posed less effect than catalyst loading on phenol degradation. Reaction temperature would significantly affect the phenol degradation: the higher of temperature, the higher of degradation rate is. The kinetic studies suggested that the heterogeneous system followed zero order kinetics and the activation energies were 81.4, 67.4 and 67.4 kJ/mol, for Co/SBA-15-Cl, Co/SBA-15-Ac, and Co/SBA-15-N, respectively.

References

[1] R. Andreozzi, V. Caprio, A. Insola, R. Marotta, Catalysis Today 53 (1999) 51–59.
[2] S. Esplugas, J. Gimenez, S. Contreras, E. Pascual, M. Rodriguez, Water Research 36 (2002) 1034–1042.
[3] M. Pera-Titus, V. Garcia-Molina, M.A. Banos, J. Gimenez, S. Esplugas, Applied Catalysis B-Environmental 47 (2004) 219–256.
[4] J.H. Sun, X.Y. Li, J.L. Feng, X.K. Tian, Water Research 43 (2009) 4363–4369.
[5] V. Kavitha, K. Palanivelu, Chemosphere 55 (2004) 1235–1243.
[6] S. Wang, Dyes and Pigments 76 (2008) 714–720.
[7] G.P. Anipsitakis, E. Stathatos, D.D. Dionysiou, Journal of Physical Chemistry B 109 (2005) 13052–13055.
[8] G.P. Anipsitakis, D.D. Dionysiou, M.A. Gonzalez, Environmental Science & Technology 40 (2006) 1000–1007.
[9] P. Shukla, S.B. Wang, K. Singh, H.M. Ang, M.O. Tade, Applied Catalysis B-Environmental 99 (2010) 163–169.
[10] Q.J. Yang, H. Choi, Y.J. Chen, D.D. Dionysiou, Applied Catalysis B-Environmental 77 (2008) 300–307.
[11] S.B. Wang, H.T. Li, Microporous and Mesoporous Materials 97 (2006) 21–26.
[12] S.B. Wang, Microporous and Mesoporous Materials 117 (2009) 1–9.
[13] X.Y. Chen, J.W. Chen, X.L. Qiao, D.G. Wang, X.Y. Cai, Applied Catalysis B-Environmental 80 (2008) 116–121.
[14] W. Zhang, H.L. Tay, S.S. Lim, Y.S. Wang, Z.Y. Zhong, R. Xu, Applied Catalysis B-Environmental 95 (2010) 93–99.
[15] Q.J. Yang, H. Choi, D.D. Dionysiou, Applied Catalysis B-Environmental 74 (2007) 170–178.
[16] P.R. Shukla, S. Wang, H. Sun, H.M. Ang, M. Tadé, Applied Catalysis B: Environmental 100 (2010) 529–534.
[17] P. Shukla, S. Wang, H. Sun, H.-M. Ang, M. Tadé, Chemical Engineering Journal 164 (2010) 255–260.
[18] D.Y. Zhao, J.L. Feng, Q.S. Huo, N. Melosh, G.H. Fredrickson, B.F. Chmelka, G.D. Stucky, Science 279 (1998) 548–552.
[19] H. Tuysuz, Y. Liu, C. Weidenthaler, F. Schuth, Journal of the American Chemical Society 130 (2008) 14108–14110.
[20] F. Xia, E. Ou, L. Wang, J.Q. Wang, Dyes and Pigments 76 (2008) 76–81.
[21] J. van der Meer, I. Bardez-Giboire, C. Mercier, B. Revel, A. Davidson, R. Denoyel, Journal of Physical Chemistry C 114 (2010) 3507–3515.
[22] T. Tsoncheva, L. Ivanova, J. Rosenholm, M. Linden, Applied Catalysis B-Environmental 89 (2009) 365–374.
[23] S.K. Ling, S.B. Wang, Y.L. Peng, Journal of Hazardous Materials 178 (2010) 385–389.
[24] X.Y. Chen, X.L. Qiao, D.G. Wang, J. Lin, J.W. Chen, Chemosphere 67 (2007) 802–808.
[25] P. Shukla, I. Fatimah, S. Wang, H.M. Ang, O. Tade Moses, Catalysis Today 157 (2010) 410–414.
[26] W. Chu, W.K. Choy, C.Y. Kwan, Journal of Agricultural and Food Chemistry 55 (2007) 5708–5713.